Author Manuscript

Author Manuscript

Author Manuscript

Author Manuscript

HHS Public Access

Author manuscript

Nat Chem Biol. Author manuscript; available in PMC 2017 March 05.

Published in final edited form as:

Nat Chem Biol. 2016 November ; 12(11): 923–930. doi:10.1038/nchembio.2171.

Overcoming Resistance to HER2 Inhibitors Through State-Specific Kinase Binding

Chris J. Novotny[1], **Sirkku Pollari**[2], **Jin H. Park**[3], **Mark A. Lemmon**[3,4], **Weijun Shen**[2,*], and **Kevan M. Shokat**[1,*]

[1]Howard Hughes Medical Institute and Department of Cellular and Molecular Pharmacology, University of California San Francisco, San Francisco, CA 94158, USA

[2] California Institute for Biomedical Research (Calibr), 11119 N. Torrey Pines Road, La Jolla, CA 92037, USA

[3] Department of Biochemistry and Biophysics and Graduate Group in Biochemistry and Molecular Biophysics, University of Pennsylvania Perelman School of Medicine, Philadelphia, PA 19104, USA

Abstract

The heterodimeric receptor tyrosine kinase complex formed by HER2 and HER3 can act as an oncogenic driver and is also responsible for rescuing a large number of cancers from a diverse set of targeted therapies. Current inhibitors of these proteins, particularly HER2, have dramatically improved patient outcomes in the clinic but recent studies have demonstrated that stimulation of the heterodimeric complex, either by growth factors or increasing the concentrations of HER2 and HER3 at the membrane, significantly diminishes their activity. In order to find an inhibitor of the active HER2/HER3 oncogenic complex we developed a panel of Ba/F3 cell lines suitable for ultra-high throughput screening. Medicinal chemistry on the hit scaffold resulted in a novel inhibitor that acts through the preferential inhibition of the active state of HER2 and as a result is able to overcome cellular mechanisms of resistance such as growth factors or mutations that stabilize the active form of HER2.

Users may view, print, copy, and download text and data-mine the content in such documents, for the purposes of academic research, subject always to the full Conditions of use:http://www.nature.com/authors/editorial_policies/license.html#terms

[*]**Corresponding Authors** Kevan M. Shokat, University of California San Francisco, 600 16th street, N512D, San Francisco, CA, 94158-2280, Phone: (415)514-0472, kevan.shokat@ucsf.edu, Weijun Shen, California Institute for Biomedical Research (Calibr), 11119 North Torrey Pines Road, suite 100, La Jolla, CA 92037, Phone: (858) 242-1018, Fax: (858)242-1001, wshen@calibr.org.
[4]Present address: Department of Pharmacology and Cancer Biology Institute, Yale University, New Haven, CT 06520

Author Contributions

C.J.N., M.A.L., W.S., K.M.S. designed research, S.P. and W.S. performed the high throughput screen and counter screens, J.H.P. co-crystalized the **2**/EGFR complex and performed the HER3 kinase assay, C.J.N. conducted cell proliferation/growth and death experiments, western blots, chemical synthesis, creation of Ba/F3 cell lines, and *in vitro* HER2 and HER3 assays. All authors analyzed data and contributed to the writing of the manuscript.

Accession Codes

The macromolecular structure has been deposited with Protein Data Bank under the accession number 5JEB.

Competing financial interests statement

The authors declare no competing financial interests

Author Manuscript Author Manuscript Author Manuscript Author Manuscript

Introduction

Signaling from the epidermal growth factor receptor (EGFR or HER) family of receptor tyrosine kinases (RTK) is dependent on a well-orchestrated series of interactions between family members to form either homo- or heterodimers[1-3]. This dimerization process allows the intracellular kinase domains to form an asymmetric dimer in which the C-terminal domain of the activator kinase binds to the N-terminal portion of the receiver kinase to stabilize it in an active conformation[4](Fig. 1a). The receiver kinase then phosphorylates tyrosine residues on the C-terminal tails of the kinases to recruit and activate downstream signaling components, most notably those involved in pro-growth and survival pathways. Because of this, the improper activation of the EGFR family of kinases, either by mutation or overexpression, is observed in a variety of cancers[5,6]. Interestingly, cell culture studies suggest that rather than causing escape from the biological mechanism of regulation, oncogenic activation alters the equilibrium between active and inactive states to favor the improper dimerization and activation of these receptors[7,89]. This dependence on dimerization is particularly evident in HER2-overexpressing breast cancers that are dependent on the presence of HER3[10].

Within the EGFR family, HER2 and HER3 are unique. HER3 is classified as a pseudokinase with only residual kinase activity, whereas HER2 has no known activating ligand but is constitutively able to dimerize with other active family members. In this way, HER2 and HER3 together form a functional RTK unit, with HER3 responding to activating ligands such as neuregulin, HER2 providing the intracellular kinase activity, and both intracellular domains providing phosphorylation sites. Additionally, HER2 and HER3 are each other's preferred heterodimerization partners and also form the most mitogenic complex among all possible EGFR family dimers[11]. Because of this co-dependence, HER3 is equally important for the formation, proliferation, and survival of HER2-overexpressing tumors[12].

Although HER2 amplification and overexpression is the most well studied means of oncogenic activation of the HER2/HER3 heterodimer, improper signaling can also be caused by secretion of the HER3 ligand NRG to stimulate HER2/HER3 heterodimers in an autocrine manner as well as by mutations in HER3 that stabilize and activate heterodimers independently of ligand[13,14]. In addition, mutations that activate the HER2 kinase domain have also been reported[15-17].

In an effort to treat these tumors, small molecule kinase inhibitors such as lapatinib or HER2-targeted antibodies such as ado-trastuzumab emtansine (T-DM1) have been developed and shown efficacy against HER2-driven cancers in the clinic[18,19]. However, recent studies have demonstrated that the presence of NRG induces resistance against currently approved HER2-targeted mono-therapies through HER2/HER3 signaling[20,21]. Additionally, inhibition of HER2/HER3 signaling at either the RTK level or of the downstream PI3K/Akt pathway releases a negative feedback loop that increases the transcription, translation, and membrane localization of HER3[22-24]. This increase in the level of HER3 causes a rebound in its phosphorylation and reactivation of the PI3K/Akt pathway even in the continued presence of lapatinib, indicating that formation of HER2/HER3 heterodimers is crucial for intrinsic cellular resistance to current HER2-targeted

Author Manuscript Author Manuscript Author Manuscript Author Manuscript

therapies[25]. This severe limitation illustrates why more effective therapies targeting the active HER2/HER3 dimer are required.

Here, we evaluated the ability of current reversible HER2 inhibitors to inhibit signaling and proliferation in cancer cell lines driven by HER2/HER3 heterodimers activated by different oncogenic mechanisms. Across several cell lines, stabilization of HER2 in the active conformation led to severely diminished activity of both lapatinib and TAK-285. We therefore aimed to identify a novel HER2/HER3 inhibitor that would preferentially target the active state of the heterodimer. Reasoning that a biochemical screen would be unable to capture the relevant cellular conformation of the fully formed transmembrane complex, we turned to a cell-based screening strategy. A high throughput screen of 950,000 small molecules against an engineered Ba/F3 cell line dependent on NRG stimulated HER2/HER3 heterodimers yielded a hit scaffold that we optimized to create a next generation HER2 inhibitor. The optimized inhibitor is capable of potently inhibiting signaling from the HER2/HER3 heterodimer regardless of the activating oncogenic mechanism.

Results

HER2/HER3 Heterodimers are Resistant to current Inhibitors

We first confirmed that the addition of the HER3 activating ligand neuregulin 1 (NRG) is able to dramatically rescue the proliferation of HER2-overexpressing breast cancer cell lines treated with the HER2 kinase inhibitors lapatinib and TAK-285 (Fig. 1b, Supplementary Results, Supplementary Fig. 1). This rescue of cell proliferation was dose dependent and effective at pM concentrations of NRG in the presence of either HER2 inhibitor at 1 μM (Fig. 1c). To determine how NRG was able to so profoundly rescue cellular proliferation, we examined a time course of HER2/HER3 signaling in SK-BR-3 cells exposed to either lapatinib, NRG, or the combination of the two. While lapatinib alone was able to rapidly and sustainably inhibit all signaling from HER2 and HER3, the addition of NRG prevented the complete inhibition of p-HER3 and all downstream signaling pathways at all time points examined (Fig. 1d). Analysis of signaling from alternative EGFR family members that could potentially contribute to this phenotype revealed that p-EGFR actually decreased in response to NRG and was still able to be inhibited by lapatinib while HER4, which is thought to function as a tumor suppressor, was undetectable in this cell line (Supplementary Fig. 3) [26,27].

The ability of NRG to rescue HER3 signaling in the presence of lapatinib could have several origins. The very weak kinase activity of HER3 itself is unlikely to be sufficient – although it is not inhibited by lapatinib. A more likely explanation is that NRG-induced heterodimerization of HER2 and HER3 stabilizes a conformation of the HER2 kinase domain that is resistant to the inhibitors tested. Both lapatinib and TAK-285 bind to the DFG in/αC out kinase conformation and occupy the back hydrophobic pocket of HER2 that is only available when the kinase domain is in an inactive conformation with the αC-helix in the characteristic ‘out’ position[28,29]. This mode of binding has the advantage of giving these inhibitors slow off-rates but could also explain their ineffectiveness in the presence of NRG. Crystal structures of EGFR family homodimers and of a HER3/EGFR kinase complex have shown that only the ‘activator’ kinase in the asymmetric dimer can retain the inactive

Author Manuscript Author Manuscript Author Manuscript Author Manuscript

conformation (Fig. 1a) [30,31]. In HER2/HER3 complexes, HER3 will adopt this position exclusively, whereas HER2 will take the 'receiver' kinase position and become stabilized in the active conformation. Thus, in a HER2/HER3 complex, the size and accessibility of the back hydrophobic pocket of the HER2 kinase domain will be greatly reduced, preventing lapatinib or TAK-285 from binding.

To determine if NRG-induced heterodimerization prevents lapatinib binding, we treated serum-starved SK-BR-3 cells with lapatinib either 15 min before or simultaneously with NRG stimulation and then rapidly examined HER2/HER3 signaling to monitor the on-rate of lapatinib in these cells. Lapatinib concentrations greater than 100 nM were sufficient to inhibit the entire RTK signaling pathway when added before NRG (Fig. 2a), i.e. in the absence of HER2/HER3 heterodimers. By contrast, lapatinib was much less effective when added simultaneously with NRG – where lapatinib would need to bind to the NRG-induced HER2/HER3 heterodimer to inhibit signaling – even at a concentration of 1 μM (Fig. 2a). A similar trend was seen in MCF-7 cells, which express modest levels of HER2 and HER3, demonstrating that this effect does not require HER2 overexpression (Fig. 2a). The same trend was also observed when cells were first treated with either NRG or vehicle for 15 min followed by 15 min of lapatinib treatment (Supplementary Fig. 5).

To assess if NRG's ability to rescue the cellular proliferation of cell lines where the HER2/HER3 dimer may be activated by alternative mechanisms, we assessed signaling and proliferation in CW-2 cells, which contain an activating mutation in the C-lobe of HER3 (E928G) and in the N-lobe of HER2 (L755S). Similar to the HER2-overexpressing cell lines, the addition of NRG rescued the viability of the CW-2 cells in a 72 h proliferation assay from both HER2 inhibitors and rescued HER2/HER3 signaling from lapatinib (Fig. 2b, c).

We next sought to determine whether this apparent resistance to lapatinib is specific to NRG-induced HER2/HER3 heterodimers or if mutations that bias HER2 towards its active conformation elicit a similar effect. We monitored HER2 and HER3 signaling 15 min after the addition of lapatinib in NCI-H1781 cells, which contain an insertion in the HER2 kinase domain at a position known to increase HER2 kinase activity[16]. As shown in Figure 2d, lapatinib, even at a concentration of 1 μM, was unable to fully inhibit signaling demonstrating that this activating mutation is sufficient to hinder lapatinib binding to HER2.

Taken together, these data argue that NRG rescues HER2/HER3 driven cells from DFG in/αC out inhibitors by stabilizing HER2 in the active conformation within HER2/HER3 heterodimers. This inability to directly target the active state of HER2 places a major limitation on the effectiveness of a majority of current HER2 inhibitors since inhibition of HER2/HER3 signaling triggers feedback loops that lead to the increased membrane expression of HER2 and HER3, which increases the number of active HER2/HER3 heterodimers that then rescue signaling and proliferation[22,23,25]. Our findings therefore argue that inhibitors that target the active HER2/HER3 heterodimer will have significant advantages, especially in situations that increase the number of active HER2/HER3 heterodimers.

Author Manuscript Author Manuscript Author Manuscript Author Manuscript

Identification of a Novel HER2/HER3 Inhibitor

In order to find a small molecule inhibitor capable of binding to the active HER2/HER3 signaling complex we developed a high throughput cellular screen using a Ba/F3 cell line engineered to be dependent on NRG-induced HER2/HER3 heterodimers. Ba/F3 cells are normally dependent on IL-3 signaling for their proliferation and survival but can be made dependent on introduced oncogenic signals[32]. We sequentially selected transduced Ba/F3 cells for populations stably expressing HER3 and then HER2. To ensure that all of the proliferative signal could be attributed to HER2/HER3 heterodimers rather than HER2 homodimers, the 9 C-terminal tyrosines in HER2 were mutated to phenylalanine (HER2YF). We then withdrew IL-3 and supplemented the media with NRG to select for NRG dependent HER2YF/HER3wt cells (2YF/3wt). The resulting 2YF/3wt cell line was completely dependent on NRG for survival and allowed us to screen for inhibitors of full-length HER2/HER3 heterodimers in their native cellular conformations using a cell viability assay (Fig. 3a). In addition to allowing us to identify potential inhibitors of active HER2, this cellular system also has the potential to uncover compounds with novel mechanisms of action against the pseudokinase HER3.

To validate the screen and test the effectiveness of counter-screening with either the same 2YF/3wt Ba/F3 cell line or the parental Ba/F3 cell line in the presence of IL-3 to remove cytotoxic primary hits, we first tested a panel of kinase inhibitors with established mechanisms of action. This panel of inhibitors demonstrated that MAPK pathway inhibitors (e.g. vemurafenib) would not score as hits in NRG-treated 2YF/3wt cells, whereas mTOR inhibitors (e.g. MLN0128) are ruled out in our toxicity counter screen, showing equal activity in the presence of either NRG or IL-3 (Supplementary Fig. 6). By contrast, HER2 and PI3K inhibitors showed a clear window for selective inhibition of NRG driven cells over IL-3 driven cells (Fig. 3b). In order to rapidly remove any hit compound that did not directly target the HER2/HER3 heterodimer, we created a separate Ba/F3 cell line dependent on the overexpression of full-length wt Axl, which also signals through the PI3K pathway. As shown in Figure 3b, this panel of Ba/F3 cell lines was suitable to segregate lapatinib from the PI3K inhibitor PIK-93.

The 48 h proliferation assay of 2YF/3wt + NRG cells was miniaturized and optimized for 1,536-well plates, which we used to screen a diverse collection of 950,000 drug-like molecules (Z’ ≥0.75). This primary screen resulted in 14,012 hits (>50% inhibition vs DMSO) that were reduced to 1,423 compounds after triplicate confirmation and the parental Ba/F3 + IL-3 counter-screen (<30% inhibition vs DMSO). These 1,423 compounds were then assayed in dose response against all three cell lines (2YF/3wt + NRG, parental Ba/F3 + IL-3, and Axl+) (Fig. 3c, Supplementary Table 1). This screening and triaging process led to the identification of three hit compounds sharing the same scaffold, exemplified by compound **1** in Fig. 3d, which reproducibly showed preferential inhibition of 2YF/3wt + NRG cell proliferation. Optimization of the hit scaffold through five iterations of analog synthesis, each consisting of approximately ten compounds, led to compound **2**, which shows a marked preference for the inhibition of the NRG driven cells over the others (Fig. 3e).

Author Manuscript Author Manuscript Author Manuscript Author Manuscript

The Cellular Activity of 2 Results from HER2 Inhibition

The specificity of compound **2** for the NRG-driven 2YF/3wt cells indicated that the compound had reasonable kinase specificity and was likely interfering with signaling at the RTK level. This was confirmed by *in vitro* profiling against a panel of kinases, with **2** only showing potent inhibition of EGFR and Abl (Supplementary Table 2, 3). To determine the mechanism of action of **2**, we evaluated its ability to interact with HER2 or HER3 using an *in vitro* kinase assay or thermofluor respectively. Compound **2** was equipotent to lapatinib against HER2 *in vitro* (Fig. 4a) and, surprisingly, was also capable of binding to HER3 (Fig. 4b). Moreover, unlike all other EGFR family inhibitors examined so far, **2** was also able to inhibit the small amount of HER3 auto-phosphorylation seen when the purified HER3 intracellular domain is clustered, indicating that it binds to the HER3 active site (Supplementary Fig. 7).

To determine how **2** is able to interact with multiple members of the EGFR family, we determined the X-ray crystal structure of **2** bound to the EGFR kinase domain (Fig. 4c, Supplementary Table 4). Although crystals were obtained with both the wild-type kinase domain and a V924R-mutated variant, the latter were optimized most readily. The V924R kinase domain crystallizes in the inactive (autoinhibited) conformation in the absence of inhibitor or when bound to the type I EGFR inhibitor erlotinib, because this mutation places a polar arginine side-chain in the middle of the hydrophobic patch used to form the asymmetric dimer required for EGFR dimerization[33,34] (Fig. 4c). Strikingly, **2** was able to stabilize the active conformation of this mutated EGFR kinase domain in crystals, as evidenced by the “in” conformation of the αC helix, which allows formation of the characteristic salt-bridge between the β3 lysine and the αC glutamate, as well as the ordered extension of the activation loop (Fig. 4c, d). This finding indicates that our hit scaffold may have a strong preference for binding and stabilizing the active conformation of EGFR family kinase domains. Interestingly, the HER3 kinase domain has only ever been crystallized in the inactive conformation and failed to crystallize after introducing mutations designed to destabilize the inactive state or in the presence of **2** [35,36]. This suggests that **2** may be stabilizing an alternate HER3 kinase domain conformation that could potentially prevent its ability to allosterically activate HER2.

In order to determine whether binding to HER2, HER3, or to both, was responsible for the anti-proliferative activity of **2,** we created a series of Ba/F3 cell lines dependent on NRG-induced HER2/HER3 heterodimers that possessed methionine gatekeeper mutations (TM) in either kinase alone (2YF/3**TM** and 2YF**TM**/HER3wt) or together (2YF**TM**/3**TM**). The methionine gatekeeper mutation has been shown to prevent lapatinib from binding to HER2 and was able to reduce the ability of **2** to bind to either kinase in isolation (Supplementary Fig. 8) [37]. Consistent with previous reports, both lapatinib and gefitinib (an EGFR inhibitor capable of inhibiting HER2 to a lesser extent) were unable to inhibit the proliferation of either Ba/F3 cell line that contained the gatekeeper mutation in HER2. Similarly, inhibition by **2** was only affected by the HER2 gatekeeper mutation, whereas the gatekeeper mutation in HER3 had little influence (Supplementary Table 5). These data indicate that the cellular activity of **2** is due to inhibition of HER2 kinase activity.

Author Manuscript Author Manuscript Author Manuscript Author Manuscript

Type I HER2 Inhibitors are Insensitive to NRG stimulation

Reasoning that a type I inhibitor of HER2 could possess the necessary attributes to inhibit signaling from the active HER2/HER3 heterodimer, we set out to further optimize the potency of our inhibitor. The crystal structure suggested that the extra-cyclic NH linker could form an intramolecular hydrogen bond with the 2-furan, which would help to stabilize the inhibitor in a conformation necessary for binding to the active kinase. The structure also suggested that limiting the charge density on the other 2-furan ring would prevent negative interactions with the kinase. With these parameters in mind, the second optimization effort led to compound **3**, which showed superior activity to lapatinib in the 2YF/3wt + NRG cells and specificity for this cell line over the others by multiple orders of magnitude (Fig. 5a, b). *In vitro* kinase profiling of **3** revealed a similar profile to **2** as well as similar potency against HER2 (Supplementary Table 6, Supplementary Fig. 9).

Consistent with our hypothesis that a potent type I inhibitor of HER2 would be unaffected by the presence of NRG, **3** showed little to no shift in its ability to inhibit the growth or signaling of HER2-overexpressing cell lines in the presence of NRG (Fig. 5c, Supplementary Fig. 10). Additionally, unlike lapatinib and TAK-285, 1 μM **3** was able to inhibit the proliferation of HER2-overexpressing cells over a dose response of NRG and was also able to induce cell death in the presence of NRG (Supplementary Fig. 11). To confirm that **3** could bind to the actively signaling HER2/HER3 heterodimer, we looked at signaling 15 min after the addition of NRG in SK-BR-3 cells either pre-treated with **3** followed by NRG stimulation or simultaneously treated with **3** and NRG. The minimal influence of NRG on the ability of **3** to inhibit all levels of signaling with or without pre-incubation, especially when compared to lapatinib (compare Fig. 5d to 2a), suggests that it is capable of binding to and inhibiting the active HER2/HER3 complex, which is not disrupted by **3** (Fig. 5d, Supplementary Fig. 13). A similar result was obtained in non-HER2-amplified MCF-7 cells and when NRG or vehicle was added prior to a dose response of **3** (Supplementary Fig. 14, 15).

Consistent with the results in the HER2-overexpressing cell lines, CW-2 cells were equally sensitive to **3** +/- NRG in both proliferation and signaling assays (Fig. 6a, b). This superior activity of **3** compared to lapatinib towards the CW-2 cells was not due solely to the L755S mutation in HER2 as a similar trend was also seen in a Ba/F3 cell line dependent on the HER3 mutant, HER2YF/HER3E928G (2YF/3EG), which can grow independently of NRG (Supplementary Fig. 17).

The ability of **3** to inhibit the activated form of HER2 was not limited to growth factor-induced heterodimers as the mutationally activated form of HER2 in NCI-H1781 cells was rapidly and fully inhibited by **3**, which translated into its ability to inhibit the proliferation of this cell line (Fig. 6c, d). To further evaluate the potential of **3** against HER2 mutants within a HER2/HER3 heterodimer, we transduced wt HER3 containing Ba/F3 cells with reported HER2 oncogenic mutants in the HER2YF construct[15,16]. The resulting cell lines contained the HER2 mutations L755S (2YF-L755S/3wt), Y772_A775 dup (2YF-YVMA/3wt), and G776del_insVC (2YF-VC/3wt) remained sensitive to **3** but showed complete resistance to lapatinib (Supplementary Table 7).

Author Manuscript Author Manuscript Author Manuscript Author Manuscript

An additional mechanism by which cancers can become dependent on HER2/HER3 dimers is through NRG mediated autocrine signaling[13]. Proliferation of the NRG autocrine dependent CHL-1 cell line was similar between lapatinib and **3** when measured at 72 h using CellTiter-Glo (Supplementary Fig. 18a). However, monitoring the growth of CHL-1 cells using microscopy showed that the anti-proliferative activity of **3** is immediate and more potent when compared to lapatinib, which takes some time to begin exerting its weaker anti-proliferative effect (Supplementary Fig. 18b).

We next examined signaling in CHL-1 cells after 24 h drug treatment and found that **3** was better able to inhibit NRG autocrine signaling in the presence of feedback, evidenced by the increasing expression of HER2 and HER3 with increasing concentration of drug (Fig. 6e). To further examine the differing abilities of **3** and lapatinib to inhibit feedback-released signaling in the NRG autocrine cells, we pre-treated CHL-1 cells with lapatinib for 24 h to induce feedback signaling, washed the cells, and then treated with a dose response of either lapatinib or **3** for an additional 24 h. Whereas the ability of lapatinib to inhibit feedback signaling was reduced as compared to the 24 h treatment by itself, **3** showed little to no shift in its ability to inhibit signaling – and showed complete inhibition at 1 μM (Fig. 6f). Similar results were obtained in FaDu cells, which are also dependent on NRG autocrine signaling (Supplementary Fig. 19).

To determine the feasibility of using **3** *in vivo*, we analyzed the pharmacokinetics after either IV or IP administration in mice (Supplementary Fig. 20). The short half-life of the inhibitor precluded a thorough test of **3** against xenografts and improving the PK properties of the inhibitor scaffold will be a focus of future optimization efforts.

Discussion

The conformational dynamics of protein kinases are critical for their function and for many of the adaptable characteristics of kinase-driven signaling pathways. Particular kinase conformations also offer access to distinctive structural features that can be exploited in the design of inhibitors to gain selectivity even among well conserved protein families. The DFG in/αC out binding inhibitor lapatinib targets the inactive state of a kinase with its benzyl ether substituent, which when combined with the quinazoline scaffold grants it exquisite selectivity for the EGFR family of kinases. What has so far been largely unappreciated is the vulnerability of this class of inhibitors to mechanisms that stabilize the active state of the targeted kinases, which lead to drug resistance as we describe here.

Our study highlights this vulnerability and demonstrates that multiple mechanisms of stabilizing the active conformation of HER2 – through mutation or protein/protein interactions – results in resistance to lapatinib. The challenge is therefore to develop a potent inhibitor of the HER2/HER3 heterodimer whose selectivity is independent of binding to the inactive state. In order to discover such an inhibitor we turned to cell-based screening that has shown a unique ability to identify novel kinase inhibitors that target the relevant conformation of a protein in its endogenous environment[38,39]. A screen of close to one million small molecules revealed a novel inhibitor whose potency and selectivity were improved through iterative rounds of medicinal chemistry. The resulting EGFR family

Author Manuscript Author Manuscript Author Manuscript Author Manuscript

inhibitor demonstrates the striking ability to inhibit the mutationally activated form of HER2 as well as NRG-stabilized HER2/HER3 signaling complexes, both of which are insensitive to the clinical inhibitor lapatinib.

While our approach sought to find a single agent that could address the challenge of inhibiting the active HER2/HER3 heterodimer, alternative strategies using the HER2 targeting antibody pertuzumab in conjunction with T-DM1 have also been shown to be efficacious. This treatment regimen would require sufficient doses of both drugs to be consistently present for activity as either agent by itself is unable to inhibit signaling or growth of HER2 driven cells in the presence of NRG[20]. Additionally, this dual antibody-based strategy would be unable to target the p95 fragment of HER2, which is associated with trastuzumab resistance[40,41] and poorer clinical outcomes[42,43].

Another potential strategy to target the NRG-stimulated HER2/HER3 heterodimers is to use the irreversible inhibitor of HER2 neratinib. However, neratinib is based on the same DFG in/αC out binding scaffold as lapatinib so while its electrophilic nature may make it more potent than lapatinib, it would also suffer from a reduced ability to initially bind to the activated form of HER2.

The last decade has seen an industrialization of kinase inhibitor discovery using purified protein kinases for both drug development and off-target assessment. In other target classes, such as GPCRs and ion channels, cell-based screens have been the rule rather than the exception and have led to a rich array of state specific modulators. Our work suggests that cell-based assays designed for kinases offer a powerful screening platform that can lead to a similar diversity in the state specificity of kinase inhibitors with the expectation that such state-specific binders will exhibit enhanced therapeutic benefit through potentially novel mechanisms of action.

Online Methods

Cell Culture and Reagents

BT-474, MCF-7, NCI-H1781, CHL-1, and FaDu cells were purchased from ATCC, CW-2 cells were purchased from Riken Cell Bank, HEK293T cells were purchased from the UCSF cell culture facility, and EcoPack-293 cells were purchased from Clontech. SK-BR-3 cells were a gift from Dr. Sourav Bandyopadhyay (UCSF) and parental Ba/F3 cells were a gift from Dr. Neil Shah (UCSF). All cell lines were maintained at 37°C and 5% CO_2. BT-474, NCI-H1781, CW-2, Axl+ Ba/F3, and 2YF/3EG Ba/F3 cells were maintained in RPMI-1640 (Gibco) + 10% FBS. MCF-7, CHL-1, FaDu, HEK293T, and EcoPack-293 cells were maintained in DMEM (Gibco) + 10% FBS. SK-BR-3 cells were maintained in McCoy's 5A (Gibco) + 10% FBS. Parental Ba/F3's were maintained in RPMI-1640 + 10% FBS supplemented with 10 ng/mL IL-3. 2YF/3wt, 2YF/3TM, 2YFTM/3wt, 2YFTM/3TM, 2YF-L755S/3wt, 2YF-YVMA/3wt, and 2YF-VC/3wt Ba/F3 cells were maintained in RPMI-1640 + 10% FBS supplemented with 6.25 ng/mL NRG.

Lapatinib and TAK-285 were purchased from Selleckchem and were aliquoted and stored as 10mM DMSO stocks at −20°C. Anti-phospho-EGFR (Y1068) (cat#3777), anti-EGFR

Author Manuscript Author Manuscript Author Manuscript Author Manuscript

(cat#4267), anti-phospho-HER2 (Y1221/Y1222) (cat#2243), anti-HER2 (cat#2165), anti-phospho-HER3(Y1289) (cat#2842), anti-HER3 (cat#12708), anti-HER4 (cat#4795), anti-phospho-Akt(T308) (cat#2965), anti-Akt (cat#2920), anti-phospho-ERK (cat#9101), anti-ERK (cat#4695), anti-phospho-S6 (S240/244) (cat#2215), anti-S6 (cat#2217), anti-phospho-4-EBP1 (T37/46) (cat#2855), anti-4EBP1 (cat#9644), anti-α-tubulin (cat#3873), and human neuregulin-1 (cat#5218) were purchased from cell signaling technologies. Mouse IL-3 (cat#PMC0034) was purchased from Gibco.

Cloning and Ba/F3 Cell Selection

Site-directed mutagenesis was performed according to standard protocols on the human HER2 and HER3 sequences in pcDNA3.1. The desired constructs were Gibson cloned into the pMSCV plasmid (Clontech) containing the puro resistance (HER3, Axl) or neo resistance (HER2) gene[44]. The sequences of all constructs were confirmed with DNA sequencing. To produce virus, EcoPack-293 cells in a 6-well plate were transfected with the desired pMSCV plasmid using lipofectamine LTX (Invitrogen) according to the manufacturer's protocol. Media was exchanged 8h after transfection. 48 h after transfection the viral supernatant was filtered through a 0.2μM filter and added to one well of a 6 well plate containing 2×10^6 Ba/F3 cells in 1 mL of RPMI media containing 40% FBS, 10 ng of IL-3, and 4 μg of polybrene (Sigma). The cells were then centrifuged at 2,000 × g for 90 min at room temperature, placed back in the incubator for 24 h, and then added to a T-75 flask containing fresh RPMI-1640 media supplemented with 10 ng/mL of IL-3 and incubated for an additional 24h.

For the 2YF/3wt cells, the parental cells were first transduced with HER3 according to the protocol above and were then spun down at 500×g for 5 min and re-suspended in media supplemented with 10 ng/mL IL-3 and 3 μg/mL puromycin (Invitrogen). Cells were maintained in these conditions for seven days, passaging as required. After seven days the cells were spun down, washed with fresh media, and then used for a subsequent round of transduction according to the protocol above with HER2YF virus. 48h after the second transduction, the cells were re-suspended in RPMI-1640 containing 10 ng/mL IL-3 and 800 μg/mL G418 (Invitrogen). The cells were maintained in these conditions for seven days, passaging as required. After seven days the cells were spun down, washed with fresh media, and then suspended in media supplemented with 10 ng/mL of NRG. Cells were maintained in these conditions for seven days to select for a NRG dependent population of 2YF/3wt Ba/F3 cells that were then maintained as described above. The same protocol was used for the 2YF-L755S/3wt, 2YF-YVMA/3wt, and 2YF-VC/3wt cell lines using the indicated constructs.

For the HER2YF/3TM, HER2YFTM/3wt, and HER2YFTM/3TM Ba/F3 cell lines, an identical protocol was used with the exception that the populations were first selected for expression of the indicated HER2 construct (G418 resistance), followed by the expression of the indicated HER3 construct (puromycin resistance).

HER2YF/3EG Ba/F3 cells were selected according to the protocol for the HER2YF/3TM Ba/F3's with the exception that no NRG was supplemented in the media during IL-3 independent selection.

Author Manuscript Author Manuscript Author Manuscript Author Manuscript

For Axl+ cells, the transduced cells were spun down at 500×g for 5 min and resuspended in media supplemented with 10 ng/mL IL-3 and 3 μg/mL puromycin (Invitrogen). Cells were maintained in these conditions for 7 days, passaging as required. After 7 days the cells were spun down, washed with fresh media, and then suspended in IL-3 free media. The cells were maintained in these conditions for 2 weeks to select for an IL-3 independent population of Axl+ driven cells.

Proliferation Assays

For adherent cell lines, cells were plated onto opaque white 96-well plates (Greiner cat#655083) and allowed to adhere overnight. The following day media was changed to fresh media that contained either DMSO or the indicated concentration of drug plus NRG (50ng/mL final concentration) as indicated. Plates were incubated at 37°C for 72h and cell viability was read out using CellTiter-Glo assay (Promega) according to the manufacturer's protocol. For Ba/F3 cell proliferation, cells, drug dilution, and any necessary growth factors (10 ng/mL IL-3 or 6.25 ng/mL NRG) were combined in a well of a 96 well plate. Plates were incubated at 37°C for 48h and proliferation was read out using CellTiter-Glo according to the manufacturer's protocol. For all normalized assays, proliferation was normalized to the DMSO control condition. All graphs were plotted in GraphPad Prism 6 and fit with a non-linear regression of the log(inhibitor) vs response with a variable slope where shown. All graphs are averages (+/- standard deviation) of biological triplicates each performed in technical triplicate unless otherwise noted.

Immunoblotting

Cells were grown in 6-well plates and treated according to the indicated conditions at which point the media was aspirated, cells were washed with 1 mL of cold PBS, which was then aspirated and the plates were frozen at −80°C. The frozen cells were thawed on the plates in a buffer containing 50mM Tris pH 7.5, 150mM NaCl, 1mM EDTA, and 1% Triton X-100 supplemented with 1x phosphatase (PhoSTOP, Roche) and 1x protease (complete-mini tablets, Roche) inhibitors. Lysates were scraped, transferred to Eppendorf tubes, and cleared by centrifugation at 20,000×g for 20 min at 4°C. The clarified lysates were transferred to chilled, clean tubes, and normalized for protein concentration by Bradford (Bio-Rad). The normalized lysates were diluted with Laemmli loading buffer, and 10μg of total protein was run on a 4-12% gradient gel (Invitrogen), which was then transferred to .45 μM nitrocellulose (Bio-Rad) and analyzed using the indicated primary antibodies according to the manufacturer's recommendations (1:1000 antibody dilution). Primary antibodies were detected using IRDye secondary antibodies (Li-Cor) according to the manufacturer's recommendations and scanned on an Odyssey imager (Li-Cor). Scanned images were cropped and assembled in Adobe Illustrator 6.

For the HER3 immunoprecipitation cells were treated the same as above but lysed in a buffer containing 20 mM Tris pH=7.5, 150mM NaCl, 1mM EDTA, and 1% Triton X-100 supplemented with 1x phosphatase (PhoSTOP, Roche) and 1x protease (complete-mini tablets, Roche) inhibitors. 1 mg of of the total protein was immunoprecipitated with the HER3 anti-body (CST, cat#12708) at 4°C overnight, followed by incubation with protein A beads (CST cat#8687) for 30 min at room temperature. The beads were washed 3x with lysis

Author Manuscript Author Manuscript Author Manuscript Author Manuscript

buffer, eluted by boiling in 3x laemmli buffer and analyzed by western blot as detailed above.

High Throughput Screening and Analysis

For compound screening, 20 nL of 1 mM compound solutions in DMSO were transferred (Echo Labcyte) into white 1,536-well plates. Subsequently, cells were seeded in 5 μL of growth medium (500 cells per well) using an automated plate filler (Kalypsys), resulting in 4 μM compound concentration. Each assay plate included neutral (DMSO only) and inhibitor (lapatinib) control wells. CellTiter-Glo Reagent (Promega, 2 μL/well) was added two days later. Luminescence signal was read after 10 minutes using an automated plate reader (ViewLux or Envision, Perkin-Elmer). The data were analyzed using the Genedata Screener software, normalized by neutral control. The percentage inhibition for each tested compound was calculated on per-plate basis, and all compounds that showed over 50% inhibition of the luminescence signal as compared to the DMSO control were picked as primary hits for triplicate confirmation. Hits confirmed with > 50% inhibition in two out of the three replicates were subsequently assayed in parental Ba/F3 +IL3 cells and non-toxic hits (< 30% inhibition in parental cells) were further assayed in dose response in 2YF/3wt + NRG, parental BaF3 +IL-3, and BaF3-Axl cells in order to identify hits that selectively inhibit the 2YF/3wt cells in the presence of NRG.

In vitro Kinome Screen

In vitro profiling of **2** at 100 nM and 1 μM and **3** at 1 μM was conducted by Nanosyn.

Real-Time Cell Proliferation Assay

CHL-1 cells were plated in clear bottom black 96-well plates (Corning cat# 3904) and allowed to adhere overnight. The following day media was changed to fresh media that contained either DMSO or the indicated concentration of compound. Confluence was measured every 2 h for 96 h using two bright field images per well taken on an IncuCyte Zoom (Essen BioScience). Data were graphed in GraphPad Prism 6 and are averages of biological duplicates, each performed in technical triplicate.

In vitro HER2 Kinase Assay

In vitro kinase assays with the HER2 kinase domain (SignalChem) were performed in triplicate as follows. To 9 μL of a 2.5x solution of kinase and substrate in reaction buffer was added 3μL of a 5x DMSO or inhibitor dilution in 10% DMSO:water. The inhibitor/kinase solution was incubated at room temperature for 10 minutes. The kinase assay was initiated by the addition of 3 μL of a 5x solution of ATP, and ran for 15 minutes. The final reaction conditions were 50mM Tris (pH7.4), 5mM $MnCl_2$, 0.01% Tween-20, 2mM DTT, 100 μM E_4Y substrate (SignalChem), 15 nM HER2, 2% DMSO, 50 μM ATP, and 1 μCi γ^{32}P-ATP. After 15 minutes, 3 μL of each reaction was pipetted onto phosphocellulose sheets (P81, Whatman) and allowed to dry. The sheets were then washed 4 × 5 min with a solution of 0.5% phosphoric acid, dried, and exposed to a phosphor screen overnight. Phosphorimaging was conducted on a Typhoon 9500, image intensities were quantified in ImageQuant 5.2, normalized to the DMSO control and plotted in GraphPad Prism 6.

Author Manuscript Author Manuscript Author Manuscript Author Manuscript

HER3 Thermofluor Assay

The HER3 gatekeeper mutation (T787M) was introduced into the HER3 tyrosine kinase domain in the pFastBac plasmid using standard protocols. Both wt and T787M HER3 were purified according to the previously published protocols[35]. Thermofluor reactions were performed in duplicate and set up as follows. 1 μL of an inhibitor or DMSO dilution in 40% DMSO:water was added to 19 μL of the HER3 kinase domain in reaction buffer. The final reaction solution contained 100 mM MOPS, 200 mM NaCl, 5% glycerol, 5 mM MgCl2, 0.1 mM DTT, 5x SYPRO Orange, 2 μM kinase, 2% DMSO and 20 μM inhibitor in the wells of a 96-well, low profile, white, PCR plate (USA scientific). The solution was pipetted up and down to mix, sealed with TempAssure clear PCR flat caps (USA Scientific), centrifuged at 500×g for 30 s, and heated in a Stratagene M×3005P RT-PCR machine from 25°C to 95°C in 0.5°C increments every 30 s after an initial incubation at 25°C for 10 min. Fluorescence was measured at the end of each 30s period with an excitation wavelength of 492 nm and an emission wavelength of 610 nm. To obtain the melting temperature, fluorescent signals were normalized to the maximum fluorescent signal for that well. Values after the well had reached a maximum signal were discarded and the signals were fit to the Boltzmann equation in Graphpad Prism 6. ΔT_m was calculated as the difference in melting temperature between the compound-treated kinase compared to the DMSO control.

Transfected HER2 Kinase Activity

The HER2 gatekeeper mutation (T798M) was introduced into the HER2 gene in pcDNA3.1 using standard protocols. HEK293T cells were transfected with the indicated pcDNA3.1 constructs of HER2 using Lipofectamine LTX according to the manufacturers protocol. 24h after transfection the media was exchanged for fresh drug containing media. After 1h of drug treatment the cells were processed for immunoblots according to the above protocol.

Cell Death Assay

Cells were plated in clear bottom, black, 96-well plates (Corning cat#3904) and allowed to adhere overnight. The following day media was changed to fresh media that contained 1x concentration of CellTox green (Promega) and either DMSO or the indicated concentration of drug +/- NRG (50ng/mL). Cells were allowed to grow for 72 h after which the number of dead cells was measured using the IncuCyte Zoom. Immediately after the 72 h read, 5 μL of 1.25% Triton X-100 was added to each well, which were then incubated at 37°C for 30 min to lyse all cells that were then counted by the IncuCyte. The percent cell death was calculated by dividing the number of dead cells counted at 72h by the number of total DNA containing cells after the detergent treatment. Values are the average of biological triplicate each performed in technical triplicate and were plotted in GraphPad Prism 6.

Crystallization and Structure Determination

$EGFR^{672\text{-}998}$/V924R protein expression and purification was performed exactly as previously described[34]. For the $EGFR\ TKD^{V924R}$/**2** structure, EGFR TKD protein was concentrated to 8 mg/ml in 20 mM Tris-HCl, pH 8.0, containing 150 mM NaCl and 2 mM DTT. Protein was co-crystallized with excess of a drug **2** (1:2 molar ratio) in a reservoir solution of 1.34M ammonium sulfate, 1.34% (v/v) PEG 400, and 0.1 M sodium acetate/

Author Manuscript Author Manuscript Author Manuscript Author Manuscript

acetic acid pH 5.5 in the hanging drop at 21°C. Crystals were cryo-protected in reservoir solution with added 20% (w/v) glycerol and flash frozen in liquid nitrogen. Diffraction data were collected at beamline 23ID-B of GM/CA@APS (Advanced Photon Source), where crystals diffracted to 3.3 Å, and were processed using HKL2000 (see Supplementary Table 2). The structure was solved by molecular replacement using Phaser with the active EGFR (WT) TKD structure (PDB 1M17) as an initial search model. Repeated cycles of manual building/rebuilding using Coot were alternated with rounds of refinement employing REFMAC and PHENIX, plus composite omit maps calculated using PHENIX. Coordinates, parameter files and molecular topology of **2** were generated by PRODRG[45]. Data collection and refinement statistics are shown in Supplementary Table 4, and structural figures were generated with PyMOL.

HER3 Autophosphorylation Assay

ErbB3-ICD$^{665\text{-}1323}$ wild-type expression and purification was performed exactly as previously described[35]. To monitor the change in autophosphorylation, 1μM ErbB3-ICD$^{665\text{-}1323}$ protein was incubated with inhibitors (varied concentrations noted in the figure) and DOGS-Ni-NTA (prepared as described in Zhang et al.[4]) in 100 mM MOPS pH 7.4, containing 200 mM NaCl, divalent cations (2 mM $MnCl_2$ plus 5 mM $MgCl_2$), 5 % glycerol, 0.1 mM DTT and 200 μM ATP for 1 hour at 25 °C, and the reactions were stopped by adding 50 mM EDTA and SDS-PAGE gel-loading buffer for rapid qualitative comparison of autophosphorylation by SDS-PAGE and immunoblotting with anti-phosphotyrosine (pY20) and anti-$(His)_5$.

Pharmacokinetic Evaluation of 3

Pharmacokinetic profiling of compound **3** was performed by Biotranex.

General Methods for Chemistry

Full experimental details and characterization data for all new compounds are included in the supplementary note.

Supplementary Material

Refer to Web version on PubMed Central for supplementary material.

Acknowledgements

We would like to thank Mitch Hull, Hung Nguyen, Megan Wogan, Jeff Janes, Drs. Peter G Schultz and Jason Roland from Calibr for technical assistance and helpful discussions. This work was supported in part by the Samuel Waxman Cancer Research Foundation (C.J.N., M.A.L., K.M.S.), R01 GM109176-01A1 (K.M.S.), a predoctoral fellowship (11PRE7670020) from the Great Rivers Affiliate of the American Heart Association (to J.H. P.), and a NIGMS Grant R01-GM099891 (to M.A. L.).

References

1. Lemmon MA, et al. The EGFR Family: Not So Prototypical Receptor Tyrosine Kinases. Cold Spring Harbor Perspectives in Biology. 2014; 6:a020768–a020768. [PubMed: 24691965]
2. Kovacs E, Zorn JA, Huang Y, Barros T, Kuriyan J. A Structural Perspective on the Regulation of the Epidermal Growth Factor Receptor. Annu Rev Biochem. 2015; 84:739–764. [PubMed: 25621509]

Author Manuscript Author Manuscript Author Manuscript Author Manuscript

3. Doerner A, Scheck R, Schepartz A. Growth Factor Identity Is Encoded by Discrete Coiled-Coil Rotamers in the EGFR Juxtamembrane Region. Chem Biol. 2015; 22:776–784. [PubMed: 26091170]
4. Zhang X, Gureasko J, Shen K, Cole PA, Kuriyan J. An Allosteric Mechanism for Activation of the Kinase Domain of Epidermal Growth Factor Receptor. Cell. 2006; 125:1137–1149. [PubMed: 16777603]
5. Schneider MR, Yarden Y. The EGFR-HER2 module: a stem cell approach to understanding a prime target and driver of solid tumors. Oncogene. 2015 doi:10.1038/onc.2015.372.
6. Yarden Y, Sliwkowski MX. Untangling the ErbB signalling network. Nat Rev Mol Cell Biol. 2001; 2:127–137. [PubMed: 11252954]
7. Brewer MR, et al. Mechanism for activation of mutated epidermal growth factor receptors in lung cancer. Proc Natl Acad Sci USA. 2013; 110:E3595–E3604. [PubMed: 24019492]
8. Wang Z, et al. Mechanistic insights into the activation of oncogenic forms of EGF receptor. Nat Struct Mol Biol. 2011; 18:1388–1393. [PubMed: 22101934]
9. Foster SA, et al. Activation Mechanism of Oncogenic Deletion Mutations in BRAF, EGFR, and HER2. Cancer Cell. 2016; 29:477–493. [PubMed: 26996308]
10. Lee-Hoeflich ST, et al. A Central Role for HER3 in HER2-Amplified Breast Cancer: Implications for Targeted Therapy. Cancer Res. 2008; 68:5878–5887. [PubMed: 18632642]
11. Tzahar E, et al. A hierarchical network of interreceptor interactions determines signal transduction by Neu differentiation factor/neuregulin and epidermal growth factor. Mol. Cell. Biol. 1996; 16:5276–5287. [PubMed: 8816440]
12. Vaught DB, et al. HER3 Is Required for HER2-Induced Preneoplastic Changes to the Breast Epithelium and Tumor Formation. Cancer Res. 2012; 72:2672–2682. [PubMed: 22461506]
13. Jaiswal BS, et al. Oncogenic ERBB3 Mutations in Human Cancers. Cancer Cell. 2013; 23:603–617. [PubMed: 23680147]
14. Wilson TR, et al. Neuregulin-1-Mediated Autocrine Signaling Underlies Sensitivity to HER2 Kinase Inhibitors in a Subset of Human Cancers. Cancer Cell. 2011; 20:158–172. [PubMed: 21840482]
15. Bose R, et al. Activating HER2 Mutations in HER2 Gene Amplification Negative Breast Cancer. Cancer Discovery. 2012; 3:224. [PubMed: 23220880]
16. Wang SE, et al. HER2 kinase domain mutation results in constitutive phosphorylation and activation of HER2 and EGFR and resistance to EGFR tyrosine kinase inhibitors. Cancer Cell. 2006; 10:25–38. [PubMed: 16843263]
17. Greulich H, et al. Functional analysis of receptor tyrosine kinase mutations in lung cancer identifies oncogenic extracellular domain mutations of ERBB2. Proc Natl Acad Sci USA. 2012; 109:14476–14481. [PubMed: 22908275]
18. Geyer CE, et al. Lapatinib plus Capecitabine for HER2-Positive Advanced Breast Cancer. N Engl J Med. 2006; 355:2733–2743. [PubMed: 17192538]
19. Verma S, et al. Trastuzumab Emtansine for HER2-Positive Advanced Breast Cancer. N Engl J Med. 2012; 367:1783–1791. [PubMed: 23020162]
20. Phillips GD, et al. Dual Targeting of HER2-Positive Cancer with Trastuzumab Emtansine and Pertuzumab: Critical Role for Neuregulin Blockade in Antitumor Response to Combination Therapy. Clin Cancer Res. 2013; 20:456. [PubMed: 24097864]
21. Wilson TR, et al. Widespread potential for growth-factor-driven resistance to anticancer kinase inhibitors. Nature. 2012; 487:505–509. [PubMed: 22763448]
22. Sergina NV, et al. Escape from HER-family tyrosine kinase inhibitor therapy by the kinase-inactive HER3. Nature. 2007; 445:437. [PubMed: 17206155]
23. Chakrabarty A, Sanchez V, Kuba MG, Rinehart C, Arteaga CL. Feedback upregulation of HER3 (ErbB3) expression and activity attenuates antitumor effect of PI3K inhibitors. Proc Nat Acad Sci USA. 2011; 109:2718. [PubMed: 21368164]
24. Chandarlapaty S, et al. AKT Inhibition Relieves Feedback Suppression of Receptor Tyrosine Kinase Expression and Activity. Cancer Cell. 2011; 19:58–71. [PubMed: 21215704]

Author Manuscript Author Manuscript Author Manuscript Author Manuscript

25. Amin DN, et al. Resiliency and vulnerability in the HER2-HER3 tumorigenic driver. Sci Transl Med. 2010; 2:16ra7.
26. Das PM, et al. Reactivation of epigenetically silenced HER4/ERBB4 results in apoptosis of breast tumor cells. Oncogene. 2010; 29:5214–5219. [PubMed: 20603612]
27. Sartor CI, et al. HER4 Mediates Ligand-Dependent Antiproliferative and Differentiation Responses in Human Breast Cancer Cells. Mol Cell Biol. 2001; 21:4265–4275. [PubMed: 11390655]
28. Aertgeerts K, et al. Structural Analysis of the Mechanism of Inhibition and Allosteric Activation of the Kinase Domain of HER2 Protein. J Biol Chem. 2011; 286:18756–18765. [PubMed: 21454582]
29. Wood ER, et al. A unique structure for epidermal growth factor receptor bound to GW572016 (Lapatinib): relationships among protein conformation, inhibitor off-rate, and receptor activity in tumor cells. Cancer Res. 2004; 64:6652–6659. [PubMed: 15374980]
30. Littlefield P, et al. Structural analysis of the EGFR/HER3 heterodimer reveals the molecular basis for activating HER3 mutations. Sci Signal. 2014; 7:ra114. [PubMed: 25468994]
31. Brewer MR, et al. The Juxtamembrane Region of the EGF Receptor Functions as an Activation Domain. Mol Cell. 2009; 34:641. [PubMed: 19560417]
32. Warmuth M, Kim S, Gu X-J, Xia G, Adrian F. Ba/F3 cells and their use in kinase drug discovery. Curr Opin Oncol. 2006; 19:55–60.
33. Jura N, et al. Mechanism for Activation of the EGF Receptor Catalytic Domain by the Juxtamembrane Segment. Cell. 2009; 137:1293–1307. [PubMed: 19563760]
34. Park JH, Liu Y, Lemmon MA, Radhakrishnan R. Erlotinib binds both inactive and active conformations of the EGFR tyrosine kinase domain. Biochem J. 2012; 448:417–423. [PubMed: 23101586]
35. Shi F, Telesco SE, Liu Y, Radhakrishnan R, Lemmon MA. ErbB3/HER3 intracellular domain is competent to bind ATP and catalyze autophosphorylation. Proc Natl Acad Sci USA. 2010; 107:7692–7697. [PubMed: 20351256]
36. Jura N, et al. Structural analysis of the catalytically inactive kinase domain of the human EGF receptor 3. Proc Natl Acad Sci USA. 2009; 106:21608–21613. [PubMed: 20007378]
37. Rexer BN, et al. Human Breast Cancer Cells Harboring a Gatekeeper T798M Mutation in HER2 Overexpress EGFR Ligands and Are Sensitive to Dual Inhibition of EGFR and HER2. Clin Cancer Res. 2013; 19:5390–5401. [PubMed: 23948973]
38. Yoshida T, et al. Identification and characterization of a novel chemotype MEK inhibitor able to alter the phosphorylation state of MEK1/2. Oncotarget. 2012; 3:1533–1545. [PubMed: 23237773]
39. Adrián FJ, et al. Allosteric inhibitors of Bcr-abl-dependent cell proliferation. Nature Chemical Biology. 2006; 2:95–102. [PubMed: 16415863]
40. Scaltriti M, et al. Expression of p95HER2, a truncated form of the HER2 receptor, and response to anti-HER2 therapies in breast cancer. J Natl Cancer Inst. 2007; 99:628–638. [PubMed: 17440164]
41. Chandarlapaty S, et al. Inhibitors of HSP90 block p95-HER2 signaling in Trastuzumab-resistant tumors and suppress their growth. Oncogene. 2009; 29:325–334. [PubMed: 19855434]
42. Sperinde J, et al. Quantitation of p95HER2 in paraffin sections by using a p95-specific antibody and correlation with outcome in a cohort of trastuzumab-treated breast cancer patients. Clin Cancer Res. 2010; 16:4226–4235. [PubMed: 20664024]
43. Sáez R, et al. p95HER-2 predicts worse outcome in patients with HER-2-positive breast cancer. Clin Cancer Res. 2006; 12:424–431. [PubMed: 16428482]
44. Gibson DG, et al. Enzymatic assembly of DNA molecules up to several hundred kilobases. Nat Meth. 2009; 6:343–345.
45. Schüttelkopf AW, van Aalten DMF. PRODRG: a tool for high-throughput crystallography of protein–ligand complexes. Acta Crystallogr D Biol Crystallogr. 2004; 60:1355–1363. [PubMed: 15272157]

Author Manuscript Author Manuscript Author Manuscript Author Manuscript

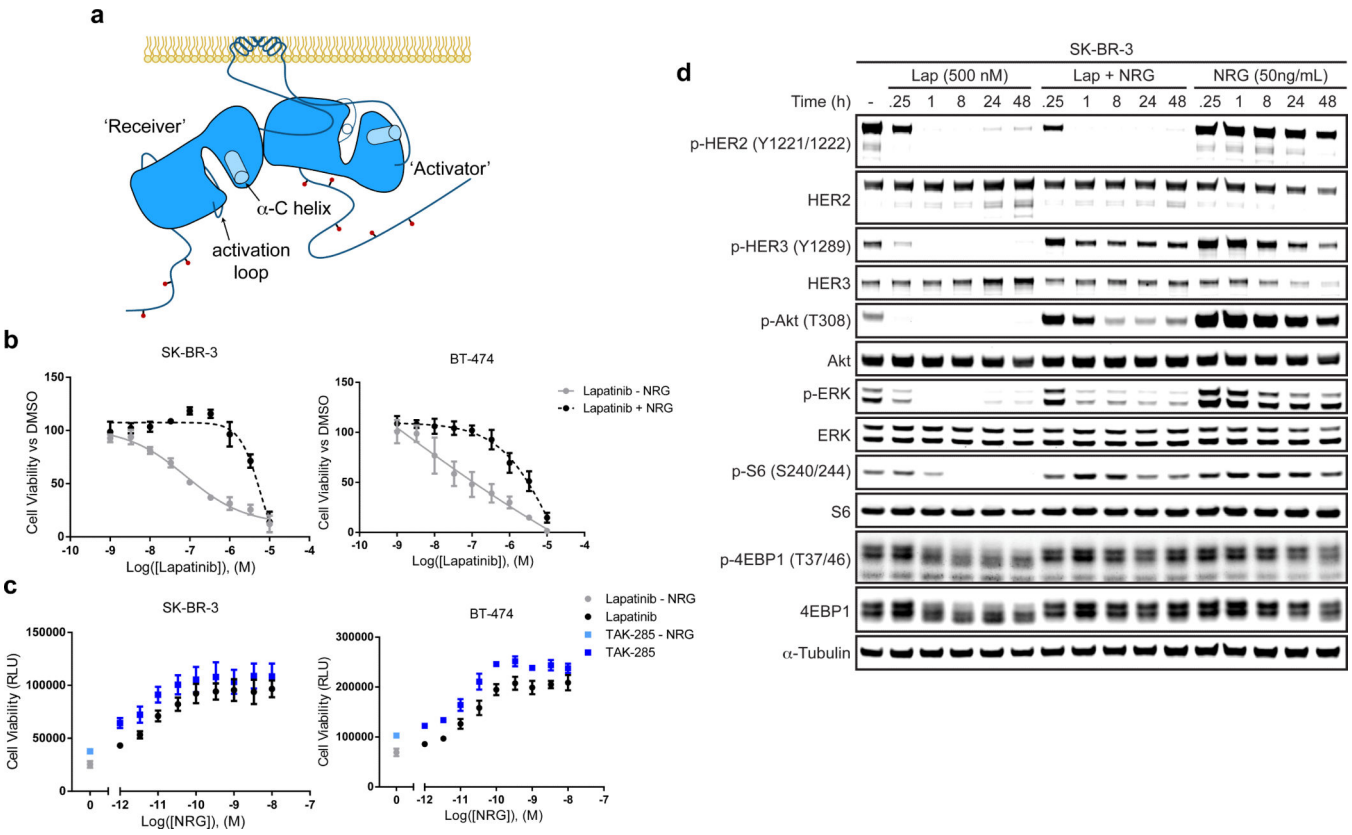

Figure 1.

NRG rescues HER2-over-expressing cancer cells from HER2 inhibitors. **a.** Cartoon schematic of the EGFR family kinase domain asymmetric dimer. The C-terminal domain of the 'activator' kinase (right) interacts with the N-terminal portion of the 'receiver' kinase (left). This interaction stabilizes the active conformation of the receiver kinase identified by the 'in' conformation of the receiver kinase's α-C helix and the ordered extension of the activation loop. The activator kinase retains the inactive conformation. **b**. 72 h proliferation of SK-BR-3 and BT-474 cells treated with a dose-response of lapatinib in the presence or absence of NRG (mean ± SD, n=3). **c.** The ability of NRG to rescue SK-BR-3 and BT-474 cell proliferation from HER2 inhibitors is dose dependent. Cells were treated with 1 μM of the indicated inhibitor in the presence of varying concentrations of NRG, and proliferation was read out after72h (mean ± SD, n=3). **d.** HER2/HER3 signaling was evaluated over a time-course in SK-BR-3 cells treated with either lapatinib, NRG, or both. The addition of NRG rescues p-HER3 and all downstream signaling at all time points examined (Full gels shown in Supplementary Fig. 2).

Author Manuscript Author Manuscript Author Manuscript Author Manuscript

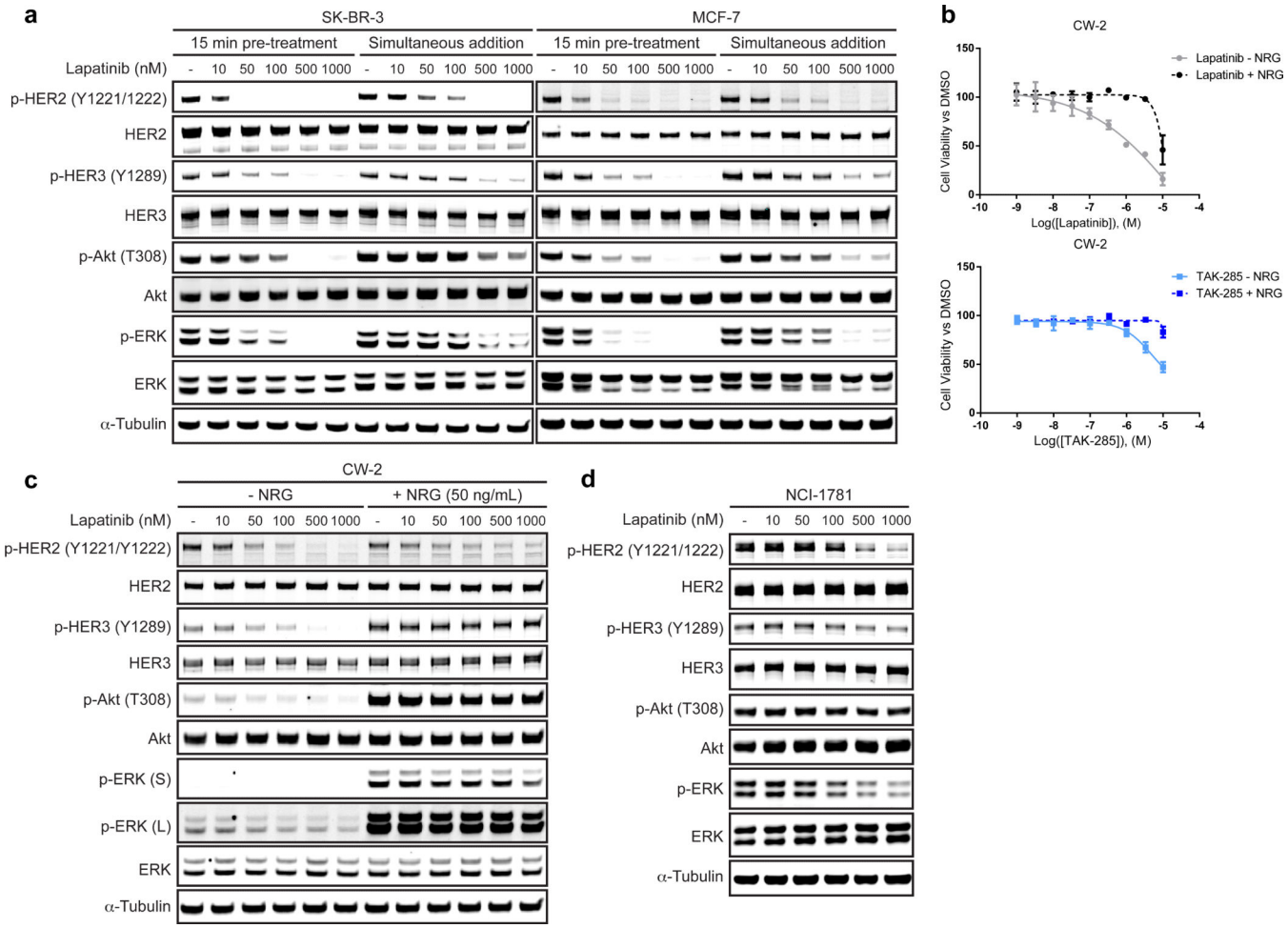

Figure 2.

Lapatinib is unable to bind to the active HER2/HER3 heterodimer. **a.** SK-BR-3 or MCF-7 cells were serum starved for 24 h and then either treated with lapatinib alone for 15 min – followed by a 15 min NRG stimulation (50ng/mL) (15 min pre-treat), or were treated with lapatinib and NRG together for 15 min (simultaneous addition). The reduced efficacy of lapatinib when simultaneously added with NRG indicates a reduced ability to bind active HER2 in HER2/HER3 heterodimers (Full gels shown in Supplementary Fig. 4a, b). **b.** NRG rescues the 72h proliferation of CW-2 cells from HER2 inhibitors (mean ± SD, n=3). **c.** CW-2 cells treated with a dose response of lapatinib in the presence or absence of NRG (50ng/mL) for 1h show that NRG rescues HER2/HER3 signaling (Full gels shown in Supplementary Fig. 4c). **d.** NCI-H1781 cells were treated with a dose response of lapatinib, and signaling was evaluated after 15 min. The short treatment time shows lapatinib does not efficiently bind to HER2 mutants biased towards the active conformation (Full gels shown in Supplementary Fig. 4d).

Author Manuscript Author Manuscript Author Manuscript Author Manuscript

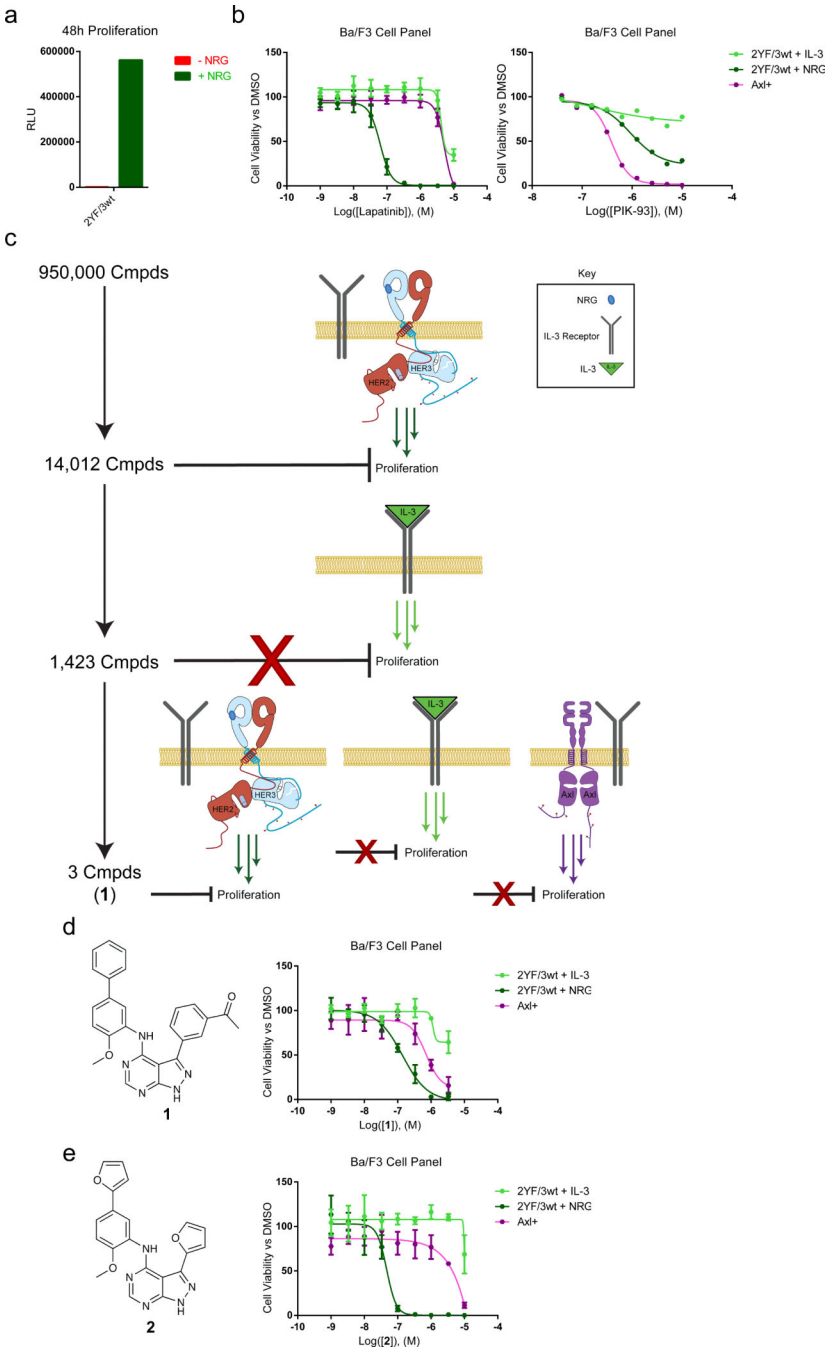

Figure 3.

Design and execution of a high-throughput screen identifies a novel HER2/HER3 inhibitor. **a**. 2YF/3wt cells were incubated in the presence or absence of NRG for 48h and proliferation was assessed by CellTiter-Glo (mean, n=1). **b**. 48h proliferation curves of the Ba/F3 cell panel show they can separate out compounds that specifically inhibit signaling at the HER2/HER3 level (lapatinib) from those that hit downstream (PIK-93) (for lapatinib mean ± SD, n=3, for PIK-93 mean, n=1). **c**. A schematic of the high throughput screen. Compounds were first screened for the ability to inhibit the proliferation of the 2YF/3wt +

Author Manuscript Author Manuscript Author Manuscript Author Manuscript

NRG cells, counter-screened against the parental cells in the presence of IL-3, and then screened in dose response against all 3 cell lines. **d.** Structure and proliferation curves for hit compound **1** against the Ba/F3 cell line panel (mean ± SD, n=3). **e.** Structure and proliferation curves for compound **2** against the panel of Ba/F3 cell lines (mean ± SD, n=3).

Author Manuscript Author Manuscript Author Manuscript Author Manuscript

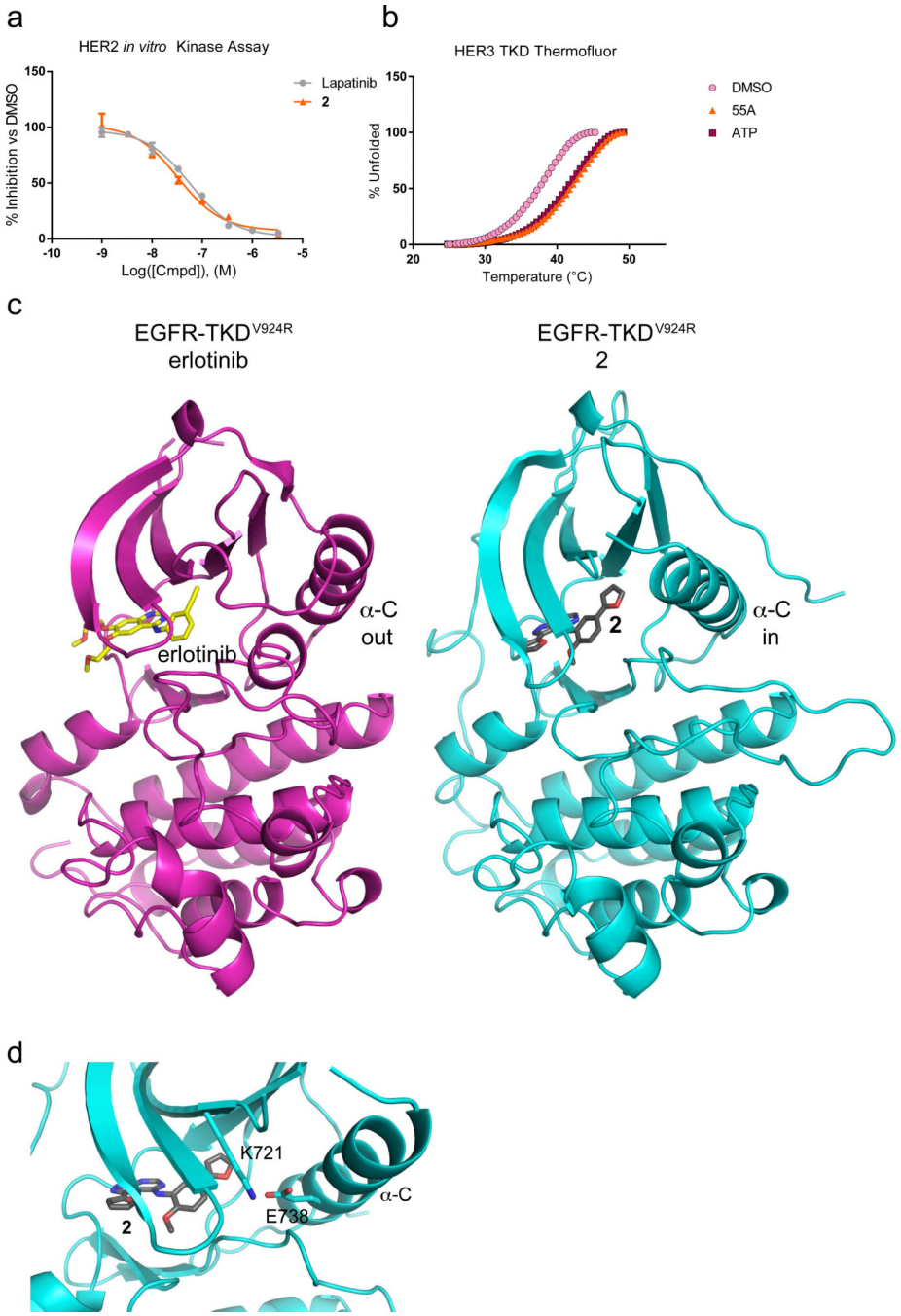

Figure 4.

Compound **2** is a selective Type I inhibitor or HER2. **a.** *In vitro* kinase assay of the HER2 kinase domain against lapatinib and **2** (mean ± SD, n=3). **b**. Thermal stabilization of the HER3 kinase domain by either **2** or ATP as determined by thermofluor (mean, n=2). **c.** The crystal structure of either erlotinib (left, PDB:4HJO) or **2** (right) bound to EGFR V924R. The kinase domain in complex with **2** has been stabilized in the active confirmation by drug binding, despite the inactivating mutation – as evidenced by the ordered extension of the activation loop and the inward positioning of the α-C helix. **d.** Magnified view of the EGFR

Author Manuscript Author Manuscript Author Manuscript Author Manuscript

V924R active site when bound to **2** shows the proximity of the β3 lysine (K721) and the glutamate (E738) in the α-C helix, which are positioned so as to make a predicted hydrogen bond.

Author Manuscript
Author Manuscript
Author Manuscript
Author Manuscript

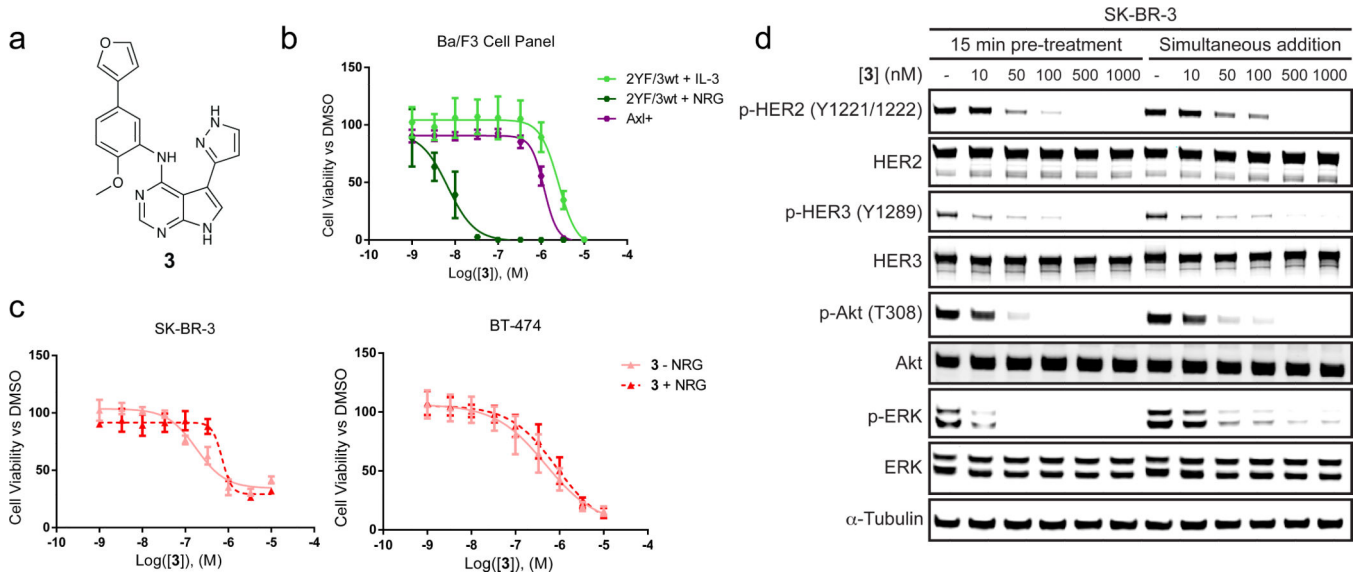

Figure 5.

A type I inhibitor of HER2 is insensitive to the presence of NRG **a.** Chemical structure of compound **3**. **b**. Proliferation curves for **3** against the Ba/F3 cell line panel (mean ± SD, n=3). **c**. 72h proliferation curves of SK-BR-3 and BT-474 cells treated with a dose response of **3** in the presence or absence of NRG indicates that **3** is insensitive to the presence of NRG in HER2-overexpressing cell lines (mean ± SD, n=3). **d**. The same assay in Fig. 2a was performed with **3** in SK-BR-3 cells (Full gels shown in Supplementary Fig. 12).

Author Manuscript Author Manuscript Author Manuscript Author Manuscript

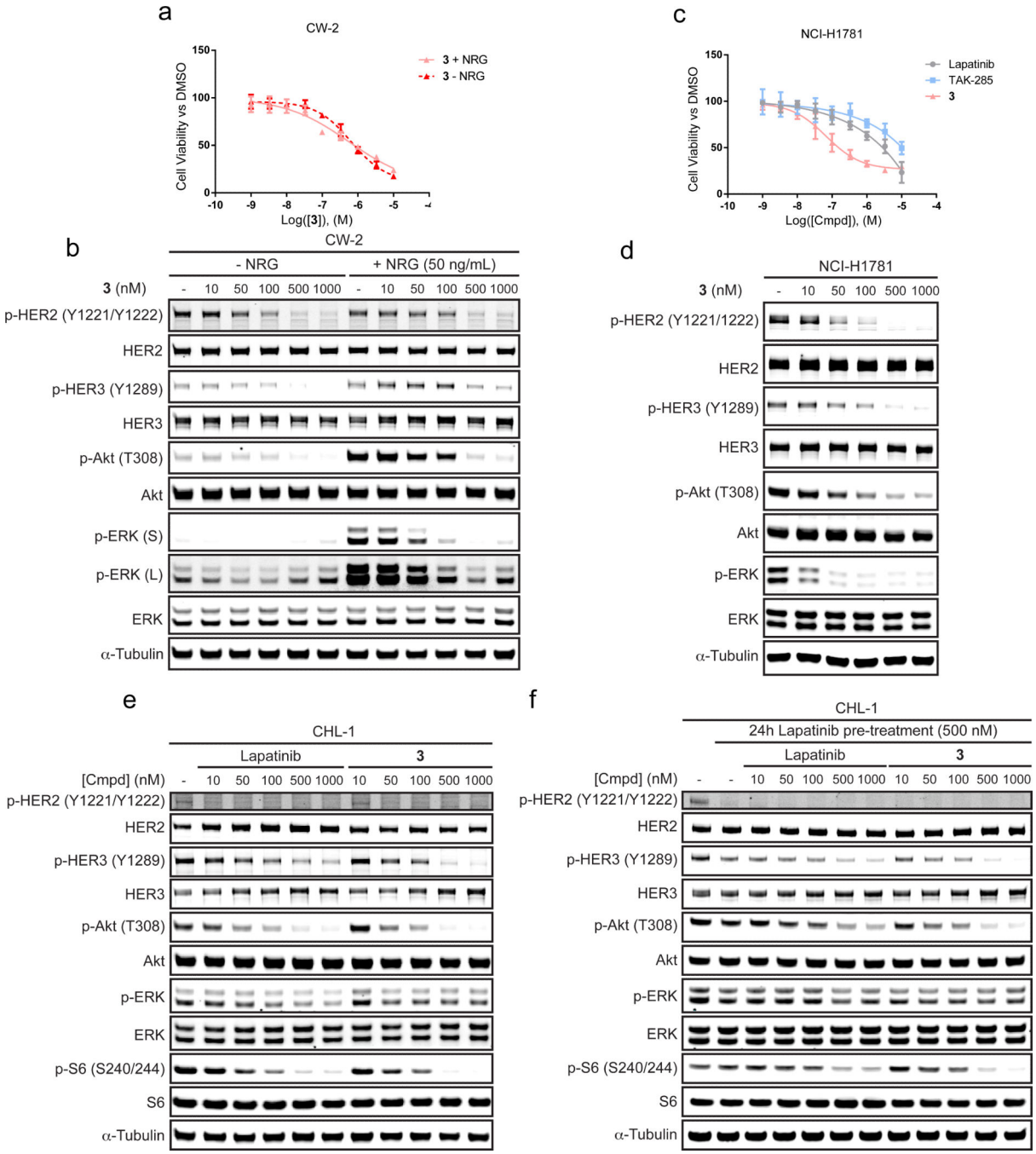

Figure 6.

3 inhibits the active HER2/HER3 heterodimer in multiple oncogenic settings. **a.** 72 h proliferation of CW-2 cells against **3** in the presence or absence of NRG (mean ± SD, n=3). **b.** CW-2 cells treated with a dose response of **3** in the presence or absence of NRG (50ng/mL) for 1h (Full gels shown in Supplementary Fig. 16a). **c.** 72 h proliferation of NCI-H1781 cells shows that they are sensitive to **3** but not to DFG in/α-C out inhibitors (mean ± SD, n=3). **d.** NCI-H1781 cells were treated with a dose response of **3** and signaling was evaluated after 15 min (Full gels shown in Supplementary Fig. 16b). **e.** HER2/HER3

Author Manuscript Author Manuscript Author Manuscript Author Manuscript

signaling was evaluated in CHL-1 cells treated with a dose response of either lapatinib or **3** for 24 h. **3** is better able to inhibit p-HER3 and thus the PI3K/Akt pathway (Full gels shown in Supplementary Fig. 16c). **f.** CHL-1 cells were treated with either DMSO or 500 nM lapatinib for 24 h. The cells were then washed and treated with a dose response of either lapatinib or **3** for an additional 24 h. Signaling shows **3** is better able to inhibit feedback activated HER2/HER3 signaling in CHL-1 cells (Full gels shown in Supplementary Fig. 16d).